HAL open science

Parametric identification of the doubly fed induction machine

Mourad Hasni, Z. Mancer, Saïd Mekhtoub, Seddik Bacha

To cite this version:

Mourad Hasni, Z. Mancer, Saïd Mekhtoub, Seddik Bacha. Parametric identification of the doubly fed induction machine. Energy Procedia, 2012, 18, pp.177-186. 10.1016/j.egypro.2012.05.029 . hal-00800325

HAL Id: hal-00800325

https://hal.science/hal-00800325v1

Submitted on 5 Sep 2019

HAL is a multi-disciplinary open access archive for the deposit and dissemination of scientific research documents, whether they are published or not. The documents may come from teaching and research institutions in France or abroad, or from public or private research centers.

L'archive ouverte pluridisciplinaire **HAL**, est destinée au dépôt et à la diffusion de documents scientifiques de niveau recherche, publiés ou non, émanant des établissements d'enseignement et de recherche français ou étrangers, des laboratoires publics ou privés.

Distributed under a Creative Commons Attribution - NonCommercial - NoDerivatives 4.0 International License

Available online at www.sciencedirect.com

SciVerse ScienceDirect

Energy Procedia 18 (2012) 177 – 186

Energy Procedia

Parametric identification of the doubly fed induction machine

Mourad HASNI[a,*], Zohir MANCER[b], Said Mekhtoub[b], Seddik BACHA[c]

[a]*Université des sciences et de la technologie Houari Boumediene Alger. E-mail : hasnimourad2001@yahoo.fr*
[b]*Ecole Nationale Polytechnique d'Alger, E-mail : mansarzohir@gmail.com*
[c]*INP Grenoble, G2Elab. Domaine Universitaire BP 45,Saint Martin d'Hères, France. E-mail : Seddik.Bacha@g2elab.inpg.fr*

Abstract

Wind Energy is a very promising energy for the future. It is well known that the power delivered by wind turbines directly coupled to the grid is not constant as a result of the wind variability. In the absence of storage systems, a fluctuating power supply produced, can lead to voltage variations in the grid and flicker. Another disadvantage of most induction machines utilized in the wind turbines is that the required reactive power varies with wind speed and time. These problems can make the use of double fed induction generators attractive for wind turbine applications.
Doubly-fed induction machines (DFIMs) are beginning to dominate the wind generation market, particularly for the larger sizes of turbine. This work is dedicated to the identification of the parametric double-fed induction machine. We propose a model of the DFIG based on the method of vector space. This model is used to validate the experimental results of identified parameters of the machine. After considering several methods of parameter identification of induction machines, provided with the results of the experiments, we are particularly interested in standardized testing. The proposed approach allows determining the electrical parameters of the machine using conventional methods static and dynamic, mechanical parameters are estimated using a digital channel, following the curve of smoothed experimental slowdown. The identified model parameters are verified by comparing their simulated stator and rotor currents responses against the measured currents. It is again observed that the estimated model responses match the measured responses well.

Keywords: wind generator; doubly fed Induction machine; Modeling; parameters Identification.

1. Introduction

Wind energy is being developed as a result of environmental problems posed by the conventional energy sources and the technological progress of wind turbines. This type of energy on the electrical network is increasingly importance in the windy areas. As a result, impact on the electricity grid, the quality of the power produced by wind turbines increases [1]. Currently the majority of wind power projects based on

* Corresponding author. Tel.:+213 771 996 837.
E-mail address: hasnimourad2001@yahoo.fr (M. HASNI)

1876-6102 © 2012 Published by Elsevier Ltd. Selection and/or peer review under responsibility of The TerraGreen Society.
Open access under CC BY-NC-ND license. doi:10.1016/j.egypro.2012.05.029

the use of double-fed induction machine. DFIG has the distinction of having two three-phase windings in stator and rotor. Using a power converter controlled by PWM to control the speed of rotation of the DFIG. This device allows the variable speed operation of DFIG and has the advantage of using a low power converter (30% of rated power supplies to the network) [2].

2. Double-fed induction generator (DFIG)

The wound rotor of the DFIG machine is usually three phase and it is housed in slots, the end of each phase is connected to a ring which is fixed on the brush rubs. This allows access to the rotor to change specifications, to connect to an assembly of power electronics such [3].

2.1. Wind systems using the DFIG

Wind turbines with variable speed electronic coupling to the rotor in Figure 1 are connected to the network by a DFIG (wound rotor). The coupling between the generator and AeroTurbine is through a mechanical speed multiplier. The stator winding is connected directly to the network and transfer the bulk of power, a power converter controlled by PWM allows varying the rotor currents of the DFIG excitation. It is important to know the parameters of the DFIG accurately, so that the control is optimal, hence the importance of identifying parametric of DFIG [4].

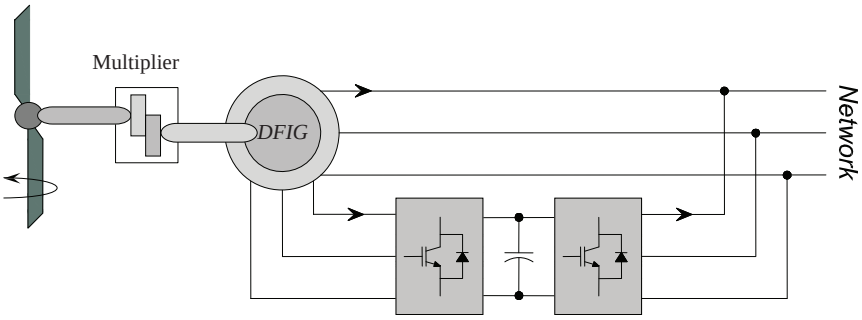

Fig. 1. Wind system based of DFIG with rotor electronic coupling.

3. Modeling of double-fed induction machine

3.1. Vector space Expression of the stator and rotor flux

The windings of the stator and rotor are represented symbolically in Figure 2. [5]

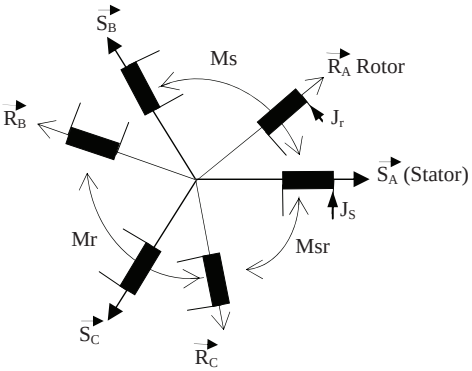

Fig.2. Definition of various inductances.

Ψsa is the flux through the coil of "SA" phase.

$$\psi_{sa}=L_s j_{sa}+M_s j_{sb}+M_s j_{sc}+M_{sr}\cos(\theta_r)j_{ra}+M_{sr}\cos(\theta_r+\frac{2\pi}{3})j_{rb}+M_{sr}\cos(\theta_r+\frac{4\pi}{3})j_{rc} \quad (1)$$

Ψra is the flux through the "RA" phase of the rotor.

$$\psi_{ra}=L_r j_{ra}+M_r j_{rb}+M_r j_{rc}+M_{sr}\cos(\theta_r)j_{sa}+M_{sr}\cos(\theta_r+\frac{4\pi}{3})j_{sb}+M_{sr}\cos(\theta_r+\frac{2\pi}{3})j_{sc} \quad (2)$$

Is also an expression of flux for the other phases in the stator and rotor have asked first:

$$M_1=M_{sr}\cos(\theta_r)\,,\ M_2=M_{sr}\cos(\theta_r+\frac{4\pi}{3}),\ M_3=M_{sr}\cos(\theta_r+\frac{2\pi}{3}) \quad (3)$$

$$\begin{bmatrix}\psi_{sa}\\ \psi_{sb}\\ \psi_{sc}\\ \psi_{ra}\\ \psi_{rb}\\ \psi_{rc}\end{bmatrix}=\begin{bmatrix}L_s & M_s & M_s & M_1 & M_3 & M_2\\ M_s & L_s & M_s & M_2 & M_1 & M_3\\ M_s & M_s & L_s & M_3 & M_2 & M_1\\ M_1 & M_2 & M_3 & L_r & M_r & M_r\\ M_3 & M_1 & M_2 & M_r & L_r & M_r\\ M_2 & M_2 & M_1 & M_r & M_r & L_r\end{bmatrix}\times\begin{bmatrix}j_{sa}\\ j_{sb}\\ j_{sc}\\ j_{ra}\\ j_{rb}\\ j_{rc}\end{bmatrix} \quad (4)$$

This relationship is written in condensed form using the inductances matrixes:

$$\begin{bmatrix}\psi_{s(a,b,c)}\\ \psi_{r(a,b,c)}\end{bmatrix}=\begin{bmatrix}[L_s] & [M_{sr}]\\ [M_{sr}] & [L_r]\end{bmatrix}\times\begin{bmatrix}j_{s(a,b,c)}\\ j_{r(a,b,c)}\end{bmatrix} \quad (5)$$

The voltage equations written using Laplace operators are summarized in matrix form, ordering the real and the imaginary parts.

$$\begin{bmatrix}v_{sD}\\ v_{sQ}\\ v_{rd}\\ v_{rq}\end{bmatrix}=\begin{bmatrix}R_s+pL_{cs} & 0 & pM & 0\\ 0 & R_s+pL_{cs} & 0 & pM\\ pM & \omega_r M & R_r+pL_{cr} & \omega_r L_{cr}\\ -\omega_r M & pM & -\omega_r L_{cr} & R_r+pL_{cr}\end{bmatrix}\times\begin{bmatrix}j_{sD}\\ j_{sQ}\\ j_{rd}\\ j_{rq}\end{bmatrix} \quad (6)$$

Is still separating the currents and their derivatives:

$$\begin{bmatrix}v_{sD}\\ v_{sQ}\\ v_{rd}\\ v_{rq}\end{bmatrix}=\begin{bmatrix}R_s & 0 & 0 & 0\\ 0 & R_s & 0 & 0\\ 0 & \omega_r M & R_r & \omega_r L_{cr}\\ -\omega_r M & 0 & -\omega_r L_{cr} & R_r\end{bmatrix}\times\begin{bmatrix}j_{sD}\\ j_{sQ}\\ j_{rd}\\ j_{rq}\end{bmatrix}+\begin{bmatrix}L_{cs} & 0 & M & 0\\ 0 & L_{cs} & 0 & M\\ M & 0 & L_{cr} & 0\\ 0 & M & 0 & L_{cr}\end{bmatrix}\times p\begin{bmatrix}j_{sD}\\ j_{sQ}\\ j_{rd}\\ j_{rq}\end{bmatrix} \quad (7)$$

3.1.1. Equations in a dq reference rotating at the speed ωx

The magnetomotive forces of the stator and the rotor, and the resulting flux and various electrical quantities of the DFIG can be represented at every moment in complex vector spaces.

Stator voltages and flux equations:

$$\begin{aligned}v_{sd}&=R_s j_{sd}+\frac{d}{dt}(\psi_{sd})-\omega_s\psi_{sq}\\ v_{sq}&=R_s j_{sq}+\frac{d}{dt}(\psi_{sq})+\omega_s\psi_{sd}\\ \psi_{sd}&=L_{cs}j_{sd}+Mj_{rd}\\ \psi_{sq}&=L_{cs}j_{sq}+Mj_{rq}\end{aligned} \quad (8)$$

Rotor voltages and flux equations:

$$\begin{aligned}v_{rd}&=R_r j_{rd}+\frac{d}{dt}(\psi_{rd})-(\omega_s-\omega_r)\psi_{rq}\\ v_{rq}&=R_r j_{rq}+\frac{d}{dt}(\psi_{rq})+(\omega_s-\omega_r)\psi_{rd}\\ \psi_{rd}&=L_{cr}j_{rd}+Mj_{sd}\\ \psi_{rq}&=L_{cr}j_{rq}+Mj_{sq}\end{aligned} \quad (9)$$

When the SA axis turn at the synchronous speed is to say, when relations $\omega_x=\omega_s$ and $\omega_s=\omega_r = g\ \omega_s$ are verified, we write:

$$v_{rd}=R_r j_{rd}+\frac{d}{dt}(\psi_{rd})-g\omega_s\psi_{rq} \tag{10}$$

$$v_{rq}=R_r j_{rq}+\frac{d}{dt}(\psi_{rq})+g\omega_s\psi_{rd} \tag{11}$$

The electromagnetic scheme is in Figure 3 below:

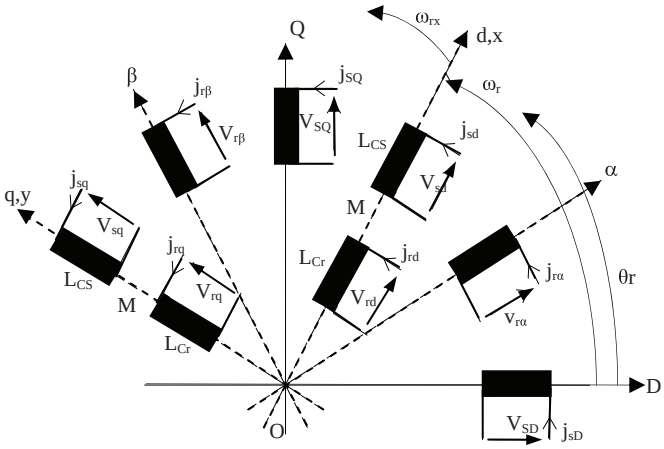

Fig. 3. Electromagnetic scheme in a reference rotating at the speed ωx.

3.2. Electromagnetic torque Expressions

The various expressions of the electromagnetic torque, written as:

$$C_{emg}=\frac{3}{2}p_0(\psi_{sd}\times j_{sq}-\psi_{sq}\times j_{sd}) \tag{12}$$

$$C_{emg}=\frac{3}{2}p_0(\psi_{rq}\times j_{rd}-\psi_{rd}\times j_{rq}) \tag{13}$$

$$C_{emg}=\frac{3}{2}\frac{M}{L_{cr}}p_0(\psi_{rd}\times j_{sq}-\psi_{rq}\times j_{sd}) \tag{14}$$

$$C_{emg}=\frac{3}{2}Mp_0(j_{sq}\times j_{rd}-j_{sd}\times j_{rq}) \tag{15}$$

3.3. Rotor dynamics equation

The sum of the torque exerted is the electromagnetic torque which is subtracted the mechanical torque resistant (Cr), dry and viscous friction torques (Cs and Cf) and eventually the ventilation torque (CV). These torques generally depend on the speed of the motor shaft.

$$J_t\frac{d\Omega_r}{dt}=C_{emg}-(C_r+C_s+C_f+C_v) \tag{16}$$

3.4. Transformation of writing equations stator and rotor

It is seeking a system of equations written in the form of state equations which the model will be like:

$$[\dot{X}] = [A][X] + [B][V] \tag{17}$$

$$[Y] = [C][X] \tag{18}$$

Or after performing the calculations:

$$\begin{bmatrix} \dot{j}_{sd} \\ \dot{j}_{sq} \\ \dot{j}_{rd} \\ \dot{j}_{rq} \end{bmatrix} = \frac{1}{\sigma} \begin{bmatrix} \frac{-R_s}{L_{cs}} & \frac{M^2\omega_r}{L_{cs}L_{cr}} & \frac{MR_r}{L_{cs}L_{cr}} & \frac{M\omega_r}{L_{cs}} \\ \frac{-M^2\omega_r}{L_{cs}L_{cr}} & \frac{-R_s}{L_{cs}} & \frac{-M\omega_r}{L_{cs}} & \frac{MR_r}{L_{cs}L_{cr}} \\ \frac{MR_r}{L_{cs}L_{cr}} & \frac{-M\omega_r}{L_{cr}} & \frac{-R_r}{L_{cr}} & -\omega_r \\ \frac{M\omega_r}{L_{cr}} & \frac{MR_r}{L_{cs}L_{cr}} & \omega_r & \frac{-R_r}{L_{cr}} \end{bmatrix} \begin{bmatrix} j_{sd} \\ j_{sq} \\ j_{rd} \\ j_{rq} \end{bmatrix} + \frac{1}{\sigma} \begin{bmatrix} \frac{1}{L_{cs}} & 0 & 0 & 0 \\ 0 & \frac{1}{L_{cs}} & 0 & 0 \\ \frac{-M}{L_{cs}L_{cr}} & 0 & 0 & 0 \\ 0 & \frac{-M}{L_{cs}L_{cr}} & 0 & 0 \end{bmatrix} \begin{bmatrix} v_{sd} \\ v_{sq} \\ 0 \\ 0 \end{bmatrix} \tag{19}$$

Therefore, if the speed ω_r is constant, on the one hand the equation of motion is not involved and the other hand the electrical equations become linear with constant coefficients therefore resolvable by simple methods. On the contrary, if the speed is not constant, the differential equations are not linear, and are practically unsolvable in most cases. For despite all the behavior of the machine during the transient, we use auxiliary calculation, which divide into two categories:

- Analog models, physical systems composed of elements combined together so that their behavior according to the same differential equations that the system we wish to solve.
- The digital computer which solves the differential equations by transforming them into finite difference equations may algebraic solution for a short time interval.

4. Identification of the DFIG

The parameter identification process is based on the following three phases [6]:

- Model selection process.
- Choice of input output signals.
- Choice of the criterion of similarity between the model and the process.

To achieve our identification, we conducted a series of experimental tests on a three-phase asynchronous machine with wound rotor, the machine specifications are: 3.5 kW, 50 Hz, U_s=380 V, I_s=8 A, U_r=240 V, I_r=9 A, 1410 tr/mn, cosφ= 0.8.

4.1. Identification of electrical parameters of DFIG by the standard tests.

The normalized electrical tests are presented in details in the standard IEC 60034 [7]. In what follows, some particular tests are presented

4.2. Identification of the rotor time constant Tr

We study the registration of the stator voltage given in Figure 4. According to the equation is that of a damped sinusoid, the response will be like: $v_{sa}(t)=Ae^{\frac{-t}{T_r}}\cos(\omega_r t+\psi)$.

This response is a system of second order in ξ reduces damping coefficient less than unity fueled by a Dirac pulse. if, $F(p)=\frac{K}{1+2\frac{\xi}{\omega_0}p+\frac{1}{\omega_0^2}p^2}$, So the impulse response is the type: $s(t)=Ae^{-\xi\omega_0 t}\sin\omega_0\sqrt{1-\xi^2}t$.

We selected two times t_1 and t_2 which correspond to passages through the points $v_{sa}(t_1)$ and $v_{sa}(t_2)$ common to the envelope and the exponential voltage $v_{sa}(t)$.

$$v_{sa}(t_1)=Ae^{\frac{-t_1}{T_r}}\ ;\ v_{sa}(t_2)=Ae^{\frac{-t_2}{T_r}} \Longrightarrow T_r=\frac{-(t_1-t_2)}{\log\left(\frac{v_{sa}(t_1)}{v_{sa}(t_2)}\right)}\ ; \qquad \text{giving} \quad T_r = 0.0732\ s$$

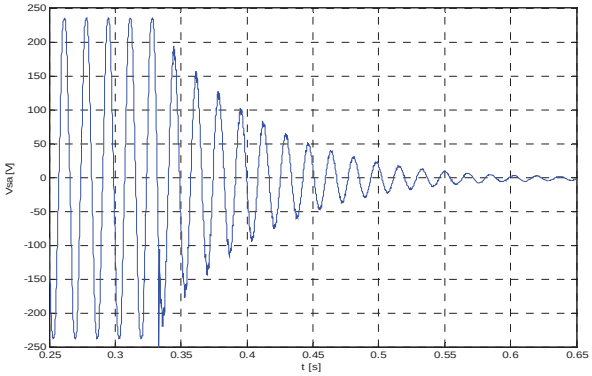

Fig. 4. Shape of the voltage across a stator phase at the opening circuit time.

4.3. Identification of mechanical parameters of the DFIG

4.3.1. Slowdown test

Knowledge of mechanical losses and the slowdown curve (figure 5), to calculate the inertia J. The equation of motion is $J\frac{d\Omega_m}{dt} = C_{emg}\text{-}C_r\text{-}C_D$ To simplify, we obtain:

$J\frac{d\Omega_m}{dt} = \text{-}C_D = -\frac{p_m}{\Omega_m}$, The value of J will be calculated from the expression:

$J=\frac{-P_m(\Omega_{r0})}{\Omega_{r0}\left/\frac{d\Omega_r}{dt}\right/_{\Omega_r=\Omega_{r0}}}$ we obtain: J=0.0259 kg.m^2

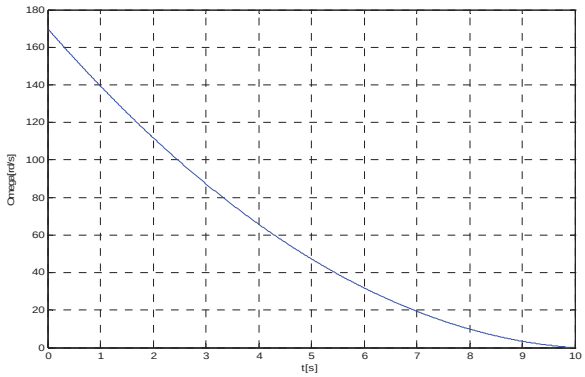

Fig. 5. Slowdown speed of the motor coupled at vacuum (smoothed curve).

4.3.2. Mathematical model of the mechanical damping torque

We propose to approximate analytically the mathematical model (20) of C_D, In its physical model (21), which is a rational polynomial approximation of first order in Ωr.

$$C_D=J\sqrt{b^2\text{-}4a(c\text{-}\Omega_r)} \qquad \text{(mathematical model)} \qquad (20)$$

$$C_D=f\Omega_r+C_s \qquad \text{(physical Model)} \qquad (21)$$

Figure 6 displays the evolution curves of mechanical damping torque of the machine, depending on the speed of mathematical and physical models, which almost overlap, which justifies the validity of the choice of the analytical structure of physical model of C_D.

The results are: $\begin{cases} f = 0.027 \text{ m.N.s} \\ C_s = 0.15 \text{ m.N} \end{cases}$

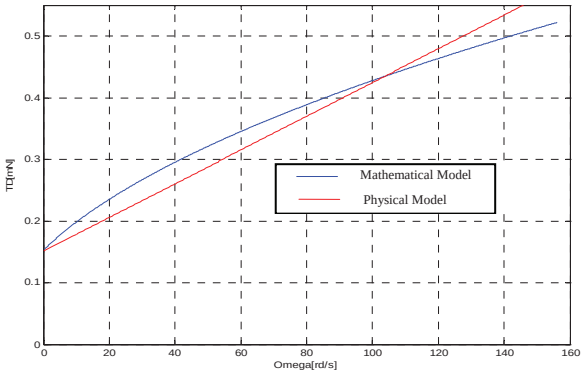

Fig. 6. Evolution of mechanical damping torque of the machine

4.4. Identification by the model method

In simple cases we can solve the problems of identification or optimization of intuitive methods. These methods become insufficient when the problem is complicated: increasing the number of parameters, introduction of constraints. It is then necessary in both cases using optimization techniques

Numerical methods are of two main types [8].:

- Direct methods which are defined as recurrence equations and lead to the solution in a finite number of steps;
- Iterative methods that assess the exact solution of the problem by successive approximations of it. It identifies three fundamental concepts of the numerical methods: that of recurrence relation, that of successive approximation and the discretization.

We introduce the need for an objective test describing the approximation measures / model. After considering different types of criterion is particularly interested in the quadratic criterion and its variants.

4.4.1. Quadratisation method

The objective is to minimize a quadratic criterion corresponding to the sum of the square of the difference between the actual output of the process to identify and that of the model obtained at each sampling instant [8,9].

4.4.2. Approximation by a quadratic polynomial interpolation

We seek a polynomial P (X) the second degree in x_1, x_2,…, x_n which interpolates f(x) on a interpolation support "simple" chosen for calculation.

The interpolation polynomial P '(X') is then:

$$P'(X') = a + \sum_{i=1}^{n} \left[b_i x_i' + \frac{1}{2} c_i x_i'^2 \right] + \sum_{\substack{1 \le i \le n \\ 1 \le j \le i-1}} d_{ij} x_i' x_j'$$

We write that P '(X-Xr) = f (X) when X takes successively the values of the chosen interpolation support. An elementary calculation gives the following results:

$$a=f(X^r)$$

$$b_i=\frac{1}{2h}\ [f(X^r+hE_i)-f(X^r-hE_i)]$$

$$c_i=\frac{1}{h^2}\ [f(X^r+hE_i)-f(X^r)+f(X^r-hE_i)]$$

$$d_{ij}=\frac{1}{h^2}\ [f(X^r+hE_{ij})-f(X^r+hE_i)-f(X^r+hE_j)+f(X^r)]$$

4.4.3. Technical of partial quadratisation

The algorithm for partial quadratisation has four phases:

a- Search for $\overline{A}$, $\overline{S}$ well as R_2.

b- In R_2, partial quadratisation and calculation of X_2^*, coordinates of the maximum of $P_2(X_2)$.

c- A calculation of X^{r+1} where θ=1.

d- Test of the condition $f(X^{r+1})>f(X^r)$.

If the relationship holds, we take X^{r+1}, value we have calculated, as the seed for the next iteration

If the relationship does not hold, we divide θ by 2. X^{r+1} is calculated and it returns on (d). The flowchart in Figure 7 summarizes the overall operations of the method applied.

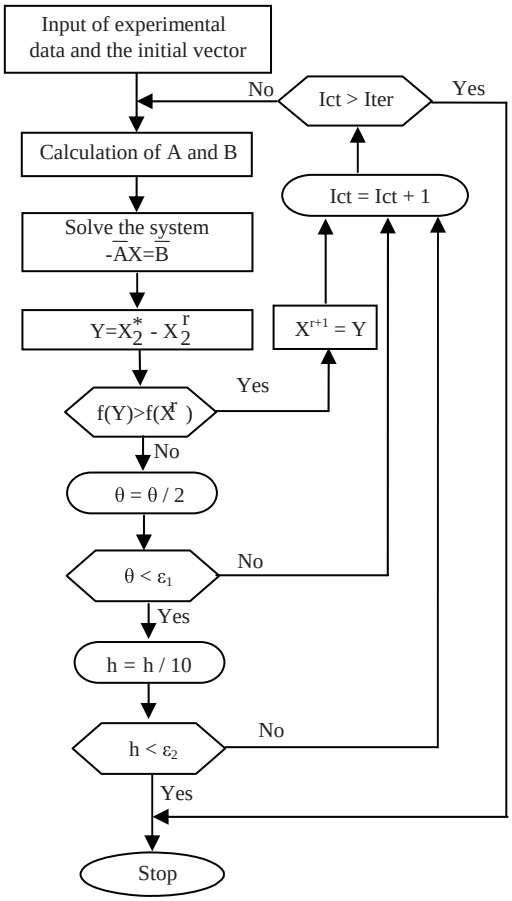

Fig. 7. General flowchart of the method.

Table 1. Identified parameters of the machine

Parameters	Values
Rs [Ω]	1,35796
Rr [Ω]	1,15243
Lsf [H]	0,00956
Lrf [H]	0,00448
Mc [H]	0,2421
Lcs [H]	0.30860
M [H]	0,14507
Ns [H]	0,09060
Nr [H]	0,05445
Lcr [H]	0,09680
Ls [H]	0,15921
Ms [H]	0,06399
Lr [H]	0,06455
Mr [H]	0,03225
Msr [H]	0,09671
σ	0,13196
K	0,98852
J [kg.m^2]	0,02590
f [m.N.s]	0,02700
Cs [m.N]	0,15000
Tr [s]	0,07320

5. Validation of the results of identification of the DFIG

5.1. Simulation results

The simulation is performed in a Matlab environment. We represent below the results obtained using the linear model of the machine we have compared with those from the experiment. They relate to the direct starting of the machine at vacuum.

Figures 8 and 9 represent the curves of measured and simulated stator voltage, the stator current and machine speed.

A comparison of the shape of the simulated signals to that obtained experimentally shows a very good agreement between the different curves with a slight difference in current amplitude, and this is due to the assumptions used in developing the model.

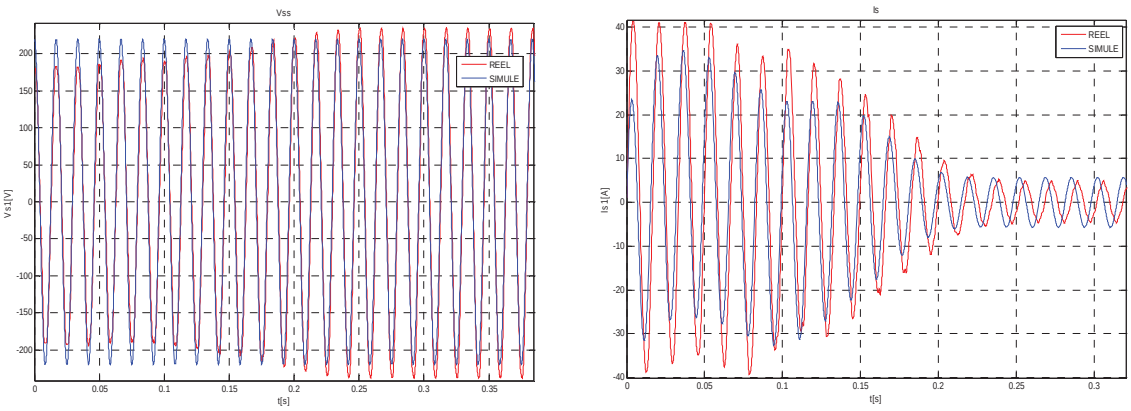

(a) (b)

Figs. 8. (a) Shape of the stator voltage of an experimental and simulated direct starting of DFIG.
(b) Shape of the stator current experimental and simulated direct starting of DFIG

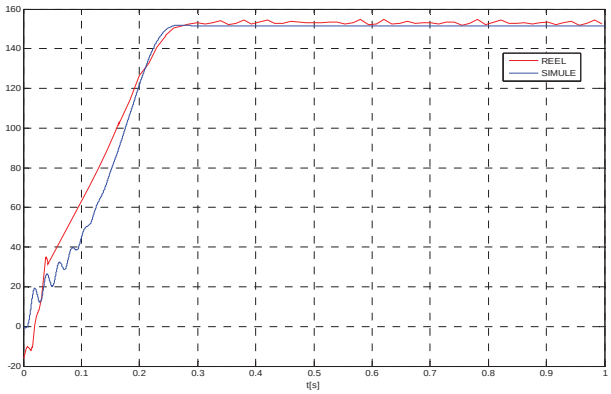

Fig. 10. Shape of the experimental and simulated speed (rd/s) of a direct starting of DFIG.

6. conclusion

The comparison of experimental results with those obtained by simulation, carried out under Matlab / Simulink, is a validation of the model of DFIG. We also addressed the issue of changes in machine parameters and poor identification and their impact on the control of DFIG.

Whatever methods of identifying the strategy that we adopt to achieve the determination of the parameters is as follows:

- Choice of parametric model,
- Finding the optimal vector,
- Checking the validity of the model.

The identification of machine parameters is a complex problem (the measurement process of signals produced by a system and building a model to represent the control system for the design and identify the model parameters from measured data based on an error criterion). It is important to note that the vector of parameters we obtained, following several methods, is a mean vector of parameters. That is to say that it is the vector which is the best compromise to represent the machine in its various types of operation.

References

[1] L.M.Fernandez, F. Jurado , J.R. Saenz. Aggregated dynamic model for wind farms with doubly fed induction generator wind turbines, *Renewable energy* No. 129-140 SD, 2008.

[2] G.K.Singh. Modeling and experimental analysis of a self-excited six-phase induction generator for stand-alone renewable energy generation, *Renewable energy* No. 1605-1621 SD, 2008

[3] M. Orabi, T. bed, M. Nakaoka, M. Z. Youssef. Efficient Performances of Induction Generator for Wind Energy Utilization. *Annual Conference No.5 IEEE*, Korea, 2004.

[4] F.Y. Ettoumi , A.H. Adane, M.L. Benzaoui, N. Bouzergui. Comparative simulation of wind park design and sitting in Algeria, *Renewable energy* No. 0960-1481 SD, 2008.

[5] P. Barret. *Régimes transitoires des machines tournantes électriques*. ESE 2, les cours de l'Ecole supérieure d'électricité Edition Eyrolles , Paris, 1981.

[6] Thomsen, S.; Rothenhagen, K.; Fuchs, F.W. Online parameter identification methods for doubly fed induction generators, *Power Electronics Specialists Conference, PESC-IEEE*, 2008, p. 2735 – 2741

[7] International Standard IEC 60034, *Rotating electrical machines, Part 4: Methods for determining based on tests, synchronous machine quantities*, Edition 3.0 September 2008.

[8] J. A. de Kock, F. S. van der Merwe, H. J. Vermeulen. Induction motor parameter estimation through an output error technique. *IEEE Tran. On Energy Conversion.* 9, (1), 1997, p. 69-75.

[9] HJ. Natke. *Application of system identification in engineering*, International Centre for Mechanical Sciences, N York, 1988.